

Development of a prototype for the analysis of multiple responses of the autonomic nervous system

*Original*

Development of a prototype for the analysis of multiple responses of the autonomic nervous system / Naranjo, D., Cattaneo, R., Mesin, L.. - In: BIOMEDICAL SIGNAL PROCESSING AND CONTROL. - ISSN 1746-8094. - STAMPA. - 70:(2021), p. 102994. [10.1016/j.bspc.2021.102994]

*Availability:*

This version is available at: 11583/2916354 since: 2021-08-03T10:11:18Z

*Publisher:*

Elsevier

*Published*

DOI:10.1016/j.bspc.2021.102994

*Terms of use:*

This article is made available under terms and conditions as specified in the corresponding bibliographic description in the repository

*Publisher copyright*

(Article begins on next page)

# Development of a Prototype for the Analysis of Multiple Responses of the Autonomic Nervous System

Daniela Naranjo<sup>a,b</sup>, Ruggero Cattaneo<sup>c</sup>, Luca Mesin<sup>a,\*</sup>

<sup>a</sup>*Mathematical Biology and Physiology, Department of Electronics and Telecommunications, Politecnico di Torino, Torino, Italy*

<sup>b</sup>*Electronics and Nanotechnology Research Department, Fundación Clínica Shaio, Bogotá, Colombia*

<sup>c</sup>*Department of Health Sciences, Università di L'Aquila, L'Aquila, Italy*

---

## Abstract

A modular hardware prototype is developed for the noninvasive acquisition, processing and transmission of biological signals to analyze the autonomic nervous system (ANS) in synchrony with the video recording of the pupil. The implementation includes 1) two noninvasive sensors, a pulse oximeter and an electrodermal activity sensor, 2) a module able to collect the information and send it to the PC via USB and 3) a graphic user interface (GUI) for visualization, synchronization and data saving. A series of experimental tests were performed to investigate the effect of different stimulations: light, dental occlusion, transcutaneous electrical nerve stimulation (TENS) and mental efforts. They indicate the reliability of the system and the importance of the joint detection of more signals for discriminating different states of the ANS. Specifically, heart rate, Galvanic response and pupil size were compared, showing some coherence in their oscillations and different discrimination capability in different conditions. Their joint detection is thus important for discriminating different states of the ANS.

*Keywords:* Pulse oximetry, Electrodermal Activity (EDA), Galvanic Skin Response (GSR), Pupillogram, Autonomous Nervous System (ANS), Transcutaneous Electrical Nerve Stimulation (TENS), Embedded systems.

---

\*Corresponding Author: Luca Mesin, Dipartimento di Elettronica e Telecomunicazioni, Politecnico di Torino, Corso Duca degli Abruzzi, 24 - 10129 Torino - Italy; Email, luca.mesin@polito.it; Phone, +39 011.090.4085

## 1. Introduction

The autonomic nervous system (ANS) is the portion of the central nervous system that controls unconscious activities, such as visceral functions and homeostasis. It is divided into two main branches, the sympathetic and the parasympathetic, the first promoting the activation of a physiological response and the other inhibiting it. The ANS is profoundly affected by emotions and somatosensory inputs and plays an important role in pain and stress modulation and perception.

Autonomic testing finds application in the clinical assessment of neurological disorders, particularly those affecting predominantly small nerve fibres [1]. Many studies have been devoted to the quantitative assessment of the ANS response, dating back to more than 3 decades [2][3][4]. However, most of the literature takes into account just one of the numerous physiological systems that are affected by the ANS in turn.

Very frequently the works that have dealt with ANS in different disorders related to its dysfunction have focused on cardio-circulatory parameters [5]. However, there are many other potential peripheral effects of ANS, that have been largely overlooked. For example, a physiological system related to the ANS can be investigated measuring skin conductance, reflecting the sweating of the sweat glands [6]. Moreover, pupil is strongly affected by the ANS [7]. The study of mydriasis and myosis (i.e., the dilation and contraction of pupil) is usually done in a different context (vestibular system). However, recent studies have indicated the possibility of characterizing the condition of the ANS in healthy or pathological conditions, by analyzing the nonlinear pupil oscillations [8][9][10][11][12][13]. In particular, the study of pupillary dynamics was considered useful for evaluating the arousal state during mental effort due to cognitive tasks [14][15] and in relation to the involvement of reward systems [16]. Furthermore, it has been suggested that the use of different ANS parameters, including pupil size, may be useful for better characterizing and quantifying the emotional component linked to the autonomous response [17]. Moreover, further evidence was provided that pupil can be used to evaluate the state of emotional arousal as well as the generic activation of the ANS [18].

One of the limitations of the study of various ANS responses is the use of different instruments for the analysis of different signals. However, it was argued that pupillogram could provide useful information for the study of the arousal state and that it would receive a valid contribution from the

38 association with signals already used for this purpose, such as skin conduc-  
39 tance and electrocortical activity [19]. These observations would involve an  
40 important expansion of the combined and synchronous study of various pa-  
41 rameters associated with pupillography to aspects not only of pathology, but  
42 also related to the emotional / affective state. Thus, important outcomes  
43 could be expected both for clinical patients and for any study involving the  
44 psychic assessment of the arousal state.

45 Only recently, more reactions of the ANS have been investigated simul-  
46 taneously [20][21]. The signals that have been often analyzed are the cardiac  
47 pulse and the variations of skin conductance. In this study, we are inter-  
48 ested in the investigation of those signals jointly with the pupil response.  
49 A modular hardware prototype is developed for the noninvasive acquisition,  
50 processing and transmission of biological signals and is synchronized with  
51 a commercial system for pupil investigation. Our present implementation  
52 includes:

- 53 • two noninvasive sensors, a pulse oximeter and an electrodermal ac-  
54 tivity sensor (both often used in the study of the responses of ANS  
55 [22][23][24]);
- 56 • a module able to collect the information and send it to the PC via USB;
- 57 • a graphic user interface (GUI) for visualization and data saving.

58 Pulse oximetry and skin conductivity are acquired in synchrony with the  
59 video recording of the patient's dilation and constriction of the pupil (ac-  
60 quired by a commercial system [25]). The system was developed keeping low  
61 the production cost and energy consumption. It was tested in experiments  
62 from healthy subjects under different stimulations: light, dental occlusion,  
63 transcutaneous electrical nerve stimulation (TENS) and computational task.

## 64 **2. Design and Implementation**

65 The recording system is shown in Figure 1. Two sensors, described below,  
66 are developed and are used together with a commercial system for pupil  
67 investigation [25].

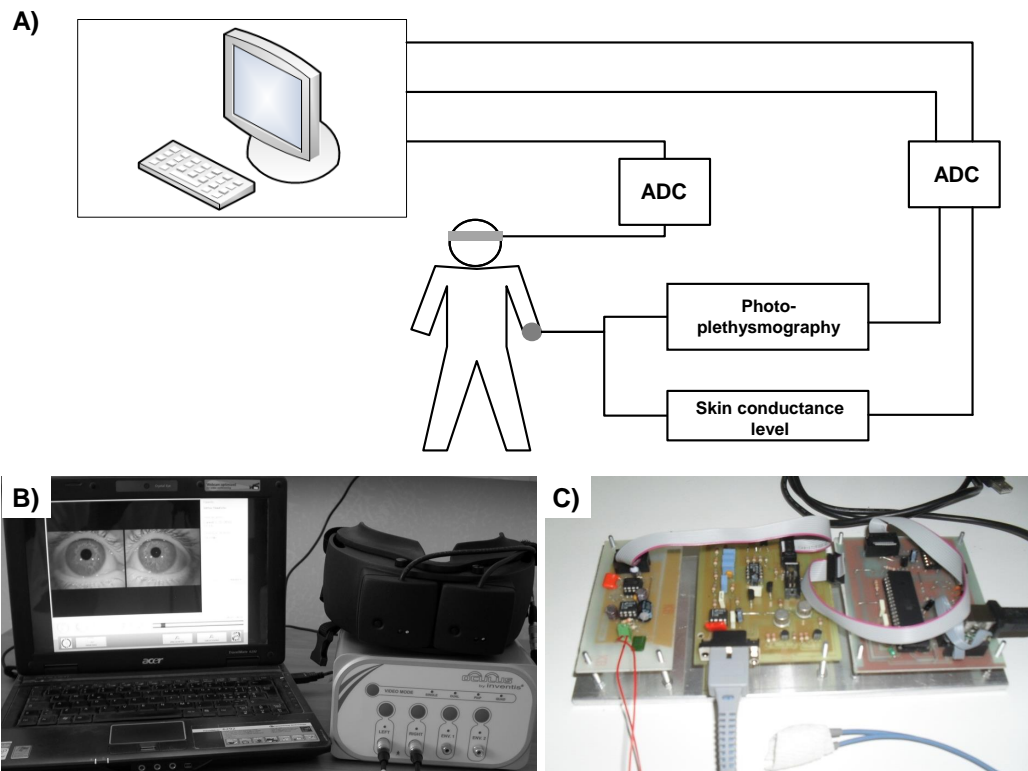


Figure 1: A) General scheme of the instrumentation used. B) Commercial system for pupil investigation [25]. C) Acquisition system recording photoplethysmogram and skin conductivity level.

68 *2.1. Design of the sensors*

69 *2.1.1. Pulse oximeter.*

70 The first sensor measures the absorption of red and infrared lights that  
71 pass through a patient's finger by light sensors. The light is generated with  
72 2 LEDs that are controlled alternately. A photodiode receives both ambient  
73 and modulated light from the LED and generates a current that is related  
74 to the oxygen saturation and the cardiac frequency [26][27][28]. The pulse  
75 oximetry signal (photoplethysmogram - PPG) has a frequency range between  
76 1 and 10 Hz. The signal is affected by the line interference (50 Hz) and  
77 the neon lamps that are usually used in offices and laboratories (giving an  
78 interference at 100 Hz), which were removed by notch filters; moreover, a  
79 high pass filter attenuated motion artifacts (notice that high performance  
80 professional oximeters are stable to ambient light and motion artifacts [29],  
81 but our low cost system had to rely on simple solutions). For the actual  
82 implementation, the sampling frequency of the PPG is 220 Hz. The circuit  
83 design is shown in Figure 2A and B.

84 *2.1.2. Skin conductivity level sensor.*

85 There are two skin resistance responses due to the electrodermal activity  
86 (EDA): the tonic and the phasic levels. The tonic level is the absolute level of  
87 resistance at a given moment in the absence of a measurable phasic response  
88 and is referred to as Skin Conductance Level (SCL). The phasic level or  
89 Skin Conductance Response (SCR) is superimposed on the tonic level and  
90 corresponds to the response to stimuli. The sum of the tonic and phasic  
91 response is the Galvanic Skin Response (GSR).

92 The skin conductance is obtained by measuring the current flow through  
93 the skin in response to a constant applied voltage. The circuit design is shown  
94 in Figure 2C. For bipolar recordings, 0.5 V is recommended [30]. For a reso-  
95 lution of  $0.01 \mu\text{S}$  (the minimum variation of the SCR [31][32]), the minimum  
96 current to be amplified is of 5 nA. The maximum input current of the ampli-  
97 fier is  $15 \mu\text{A}$  (maximum SCR and SCL), therefore the transimpedance of  
98 the circuit must be of  $333 \text{ k}\Omega$ . This circuit has two independent outputs that  
99 allow the analysis of each component separately. The sampling frequency is  
100 170 Hz.

101 *2.2. Digital processing of the signal and transmission*

102 The information coming from the analogue sensors was converted into  
103 digital form, acquired, pre-processed and transmitted via USB to a PC. The

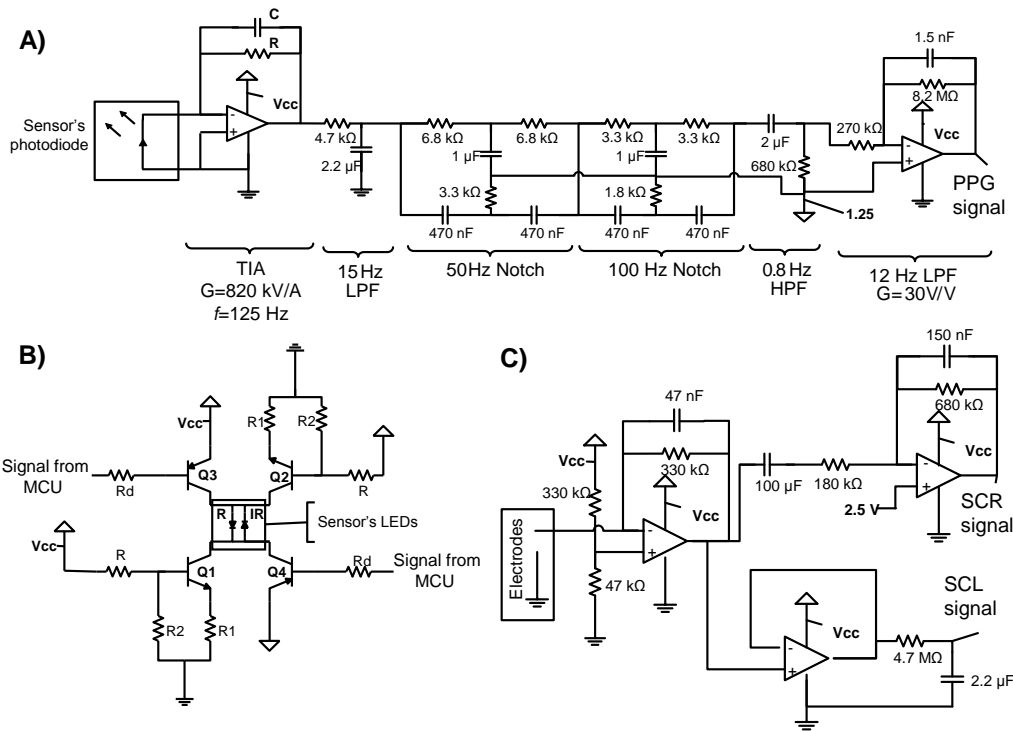


Figure 2: A) Schematic of the photoplethysmograph. B) Schematic of the LEDs driver. The signal from the microcontroller unit (MCU) controls which of the 2 LEDs is ON. C) Schematic of the skin conductance sensor. The 2 outputs are for the Skin Conductance Response (SCR) and the Skin Conductance Level (SCL).

104 microcontroller Atmel ATmega 16 accomplished these tasks [33][34]. Such a  
 105 microcontroller was chosen as it is cheap and it has a high speed, a small code  
 106 size and an analog multiplier (which can be used to implement digital filters).  
 107 Its most important characteristics are listed in Table 1. The connection of  
 108 the microcontroller to the system is shown in Figure 3. Notice that the  
 109 internal 10 bit ADC was used for sampling the skin conductance, whereas an  
 110 external 16 bits analog-to-digital converter (ADC) was included to sample the  
 111 PPG (the considered external ADC is AD7715, which is a 16-bit Sigma-Delta  
 112 ADC that can be interfaced with microcontrollers using the Serial Peripheral  
 113 Interface, SPI).

114 The red and infrared lights for the pulse oximetry sensor must be ON in  
 115 different cycles: the signal period was 1 ms, with a duty cycle of 0.25 and  
 116 the phase between the two lights was 0.5 ms. The state of the LEDs was  
 117 controlled using timer interrupt. An average filter (of 5 samples for pulse  
 118 oximetry and 20 samples for the Galvanic skin response) was implemented in  
 119 the microcontroller to remove experimental noise from the recorded signals  
 120 (the sampling frequency was about 5 kHz, so that there was sufficient time  
 121 to process the acquired data to produce a low pass filtered sample to be  
 122 acquired). The filtered samples were then transmitted to the PC with the  
 USART, which was interfaced with a USB transceiver.

Parameter	Value
Maximum Speed	16 MHz
Operating voltage	2.7 V - 5.5 V
Power consumption	Active: 1.1 mA Idle: 0.35 mA Power-down: < 1 $\mu$ A
Flash Memory	16 KB
EEPROM	512 B
Internal SRAM	1 KB
ADC Channels	8
ADC resolution	10 bits
ADC speed (max. resolution)	200 kbps
Timers max. resolution	16 bits
Serial communication	USART SPI Two-wire Serial

Table 1: General properties of the Atmega16 [33].

123  
 124

To manage the data, a software interface was developed in Visual Basic,

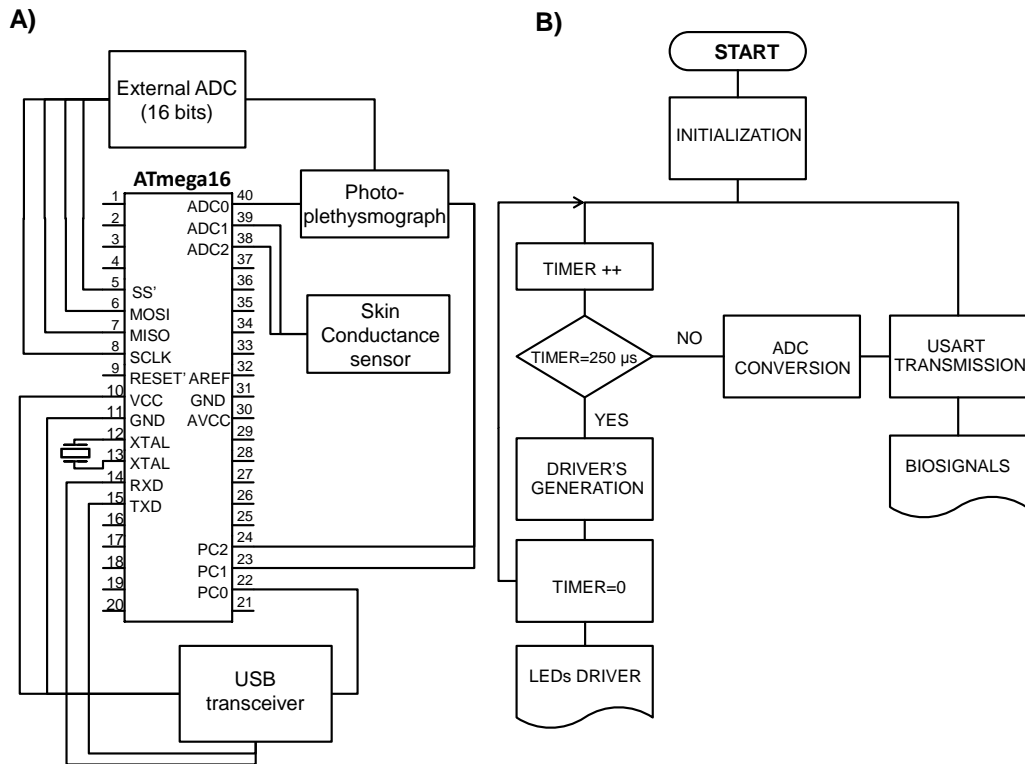


Figure 3: A) General schematic of the digital processing unit. B) Microcontroller general flow diagram.

125 with the following main functions.

- 126 • Registration of patient's information. The user should also be able to
- 127 import the information from the database of pupillograms.
- 128 • Visualization of the signals. The charts update constantly to show the
- 129 signals while they are being acquired.
- 130 • Storage of the signals. The information was stored in a file. This file
- 131 contains the patient's information, the starting time of the acquisition,
- 132 the time of each sample and the samples of the signals.

### 133 **3. Experimental tests**

#### 134 *3.1. Signal acquisition*

##### 135 *3.1.1. Instrumentation.*

136 Images of the pupils were acquired by the Oculus system (Inventis srl,  
137 Padova, Italy), using two infrared CCD cameras (resolution 720x576 pixels,  
138 256 grey levels) mounted on a light helmet (1.5 kg), with sampling frequency  
139 of 25 frame/s. The eyes were illuminated with an infrared diode with 880  
140 nm of wave-length; moreover, during experiments on pupil dynamics under  
141 constant light conditions, illumination was provided by a yellow-green LED  
142 with 740 nm of wave-length.

143 Pulse oximetry and variations of sweat were monitored with the system de-  
144 scribed in the previous sections, considering the PPG and the GSR time  
145 series.

##### 146 *3.1.2. Synchronization of the signals.*

147 The software of the considered system for pupil investigation [25] does not  
148 allow any kind of modifications or access. Therefore, the synchronization of  
149 the signals was done by registering the precise moment in which the system  
150 started recording. The signals were synchronized with a resolution of 10 ms.  
151 Given that the sampling period of the pupillogram was 40 ms, this resolution  
152 is enough.

##### 153 *3.1.3. Experimental set up.*

154 The subjects were sitting in a high-back chair. The environment was kept  
155 at a constant temperature of 21°C. Visual predominance was determined.  
156 The acquisition system was then connected to the patient's non dominant  
157 hand. The helmet was applied and was maintained until the end of the  
158 recording. This phase took about 4 minutes.

159 The correct procedure and execution of tests was first explained to the  
160 subjects. Then, they were asked for brief tests to make sure that the instruc-  
161 tions were well understood. This phase took about 2 minutes.

162 Two operators worked within the experimental set. The first took care  
163 of the subject (pretest and test instructions, helmet handling, check of the  
164 correctness of execution), the second controlled hardware and software.

165 *3.1.4. Experiments.*

166 One minute long acquisitions were obtained (after approval by the Inter-  
167 nal Review Board of Politecnico di Torino) from 8 young, healthy subjects  
168 (age  $25.1 \pm 1.1$  years; 6 females, 2 males) in different stationary conditions  
169 (separated by 5 minutes rest), which require a different involvement of the  
170 sympathetic and of the parasympathetic control: neutral position of the jaw  
171 (rest position: RP) and habitual dental occlusion (HDO)<sup>1</sup>, in light or dark-  
172 ness condition; moreover, a test was performed during a computational task,  
173 which was assumed to induce a detectable stress of the subject. These 5  
174 conditions (RP in light and darkness, HDO in light and darkness and com-  
175 putational task in darkness) were performed before, during and after the ap-  
176 plication of low-frequency TENS (5 minutes duration), which was expected  
177 to induce relaxation.

178 *3.2. Signal processing and results*

179 *3.2.1. Pre-processing of recorded data.*

180 Pupillometric recordings were processed through the algorithm of strongly  
181 connected components [35] to measure frame by frame the area of the pupil,  
182 expressed as the number of pixels covering it. The area of the pupil was then  
183 low pass filtered under 2 Hz (non-causal, zero-phase, Butterworth filter of  
184 order 2).

185 The local maxima in the PPG were used to identify the heartbeats, from  
186 which the heart rate (HR) was estimated. The GSR was low pass filtered  
187 under 2 Hz.

188 The mean and standard deviation (STD) were computed for the three  
189 following signals: pupillogram, HR and GSR. Moreover, the linear trend was  
190 estimated as a basic indicator of the evolution in time of the signals (the trend  
191 was defined as the slope of the interpolation line of the data after scaling the  
192 time to range between 0 and 1 and normalizing the time series to have zero  
193 mean and unit STD). These indexes were used as descriptors of the signals in  
194 the different experimental conditions. The two-sided Wilcoxon signed rank  
195 test (considering paired data) was then applied to investigate differences of  
196 each of the indexes in specific pairs of conditions of interest, after pooling

---

<sup>1</sup>During dental occlusion, the effect of muscle fatigue and the massive involvement of the autonomic system were excluded by avoiding prolonged teeth clenching. Subjects were asked to swallow and then to contact the teeth lightly without clenching. Attention was paid to check the activity of mimic muscles.

197 data: RP in darkness compared to the computational task, RP compared to  
198 HDO (in darkness), pre-TENS compared to TENS or post-TENS conditions.  
199 The significance level was set to  $p < 0.05$ .

### 200 3.2.2. Results.

201 Examples of recorded signals are shown in Figure 4. The pupil shows an  
202 irregular oscillatory behavior, as also the HR. There is a decreasing trend in  
203 both HR and GSR, as if the subject was relaxing. The figure shows also the  
204 spectral coherence of the pupillogram and the HR at frequencies lower than  
205 1 Hz. The two signals were found to be coherent in subjects under control  
206 breathing conditions, where a respiratory component was visible in both the  
207 pupillogram and the HR [7]. Here, the considered normal breathing and the  
208 short acquisitions resulted in significant coherence (over 0.5) only in a few  
209 subjects and conditions.

210 The significance of the differences of indexes extracted from the signals  
211 recorded in different conditions is shown in Table 2. Different indexes have  
212 a greater discriminatory value comparing different conditions:

- 213 • an index from the HR showed the maximal significance (i.e., minimum p  
214 value) in discriminating computational task and RP in darkness (which  
215 can be considered as a rest state);
- 216 • indexes estimated from the pupillogram had the maximal significance  
217 in distinguishing light and darkness, RP and HDO, or pre-TENS and  
218 TENS conditions;
- 219 • indexes extracted from GSR were the most statistically different in the  
220 conditions pre-TENS versus post-TENS and TENS versus post-TENS.

221 Specifically, HR and mean pupil size increased when comparing computa-  
222 tional task with RP in darkness (due to the mental stress induced by the  
223 task). The subject started sweating during the computational task, as indi-  
224 cated by the high positive trend of GSR. Pupil was the only system showing  
225 significant differences between HDO and RP: pupil size increased as a result  
226 of HDO stimulation [8][9][10]. Moreover, it was the only system showing  
227 significant differences comparing light and darkness conditions (obviously,  
228 increasing the diameter in darkness).

229 Pupil also indicated the relaxation induced by TENS (there is a significant  
230 reduction of pupil size during and after the application of TENS). On the

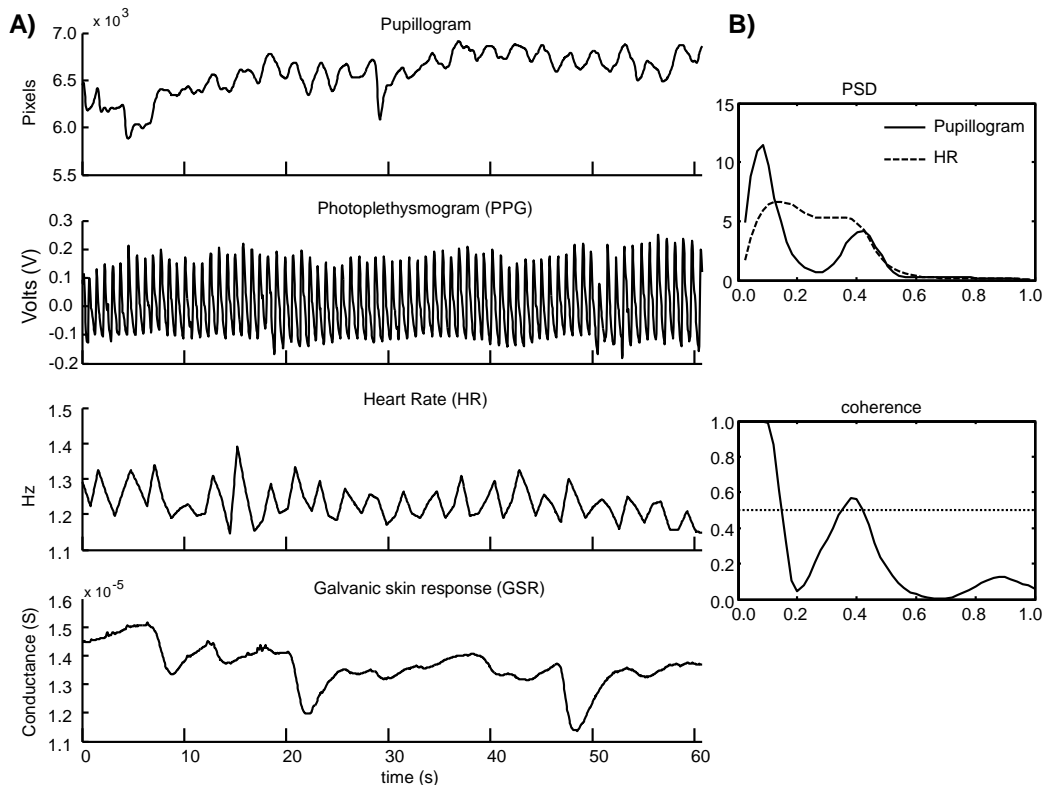


Figure 4: A) Example of data (pupillogram, PPG from which the HR is obtained, GSR), with the subject at rest position of the jaw in darkness. Power spectrum densities (PSD) of pupillogram and heart rate (using Welch’s overlapped segment averaging estimator, considering 8 segments with 50% overlap) and magnitude squared coherence.

231 other hand, GSR increased during and after TENS, with respect to the pre-  
 232 TENS condition. Possibly, this was due to an accumulation of sweat during  
 233 the experiment, as the sensors were kept fixed for all its duration.

#### 234 4. Discussion

235 The ANS controls many different visceral functions, including heart rate,  
 236 perspiration, digestion, salivation, respiratory rate, pupillary dynamics, mic-  
 237 turition (urination), sexual arousal, breathing and swallowing. The joint  
 238 acquisition of different autonomic responses could be useful for a deeper in-  
 239 sight into ANS physiology and pathology. For example, the study of the  
 240 autonomic response is important in the following situations [36]:

- 241 • sympathetic and parasympathetic lesions after surgical procedures;
- 242 • drug's collateral effects;
- 243 • diagnosis and follow up of ANS diseases;
- 244 • poisoning;
- 245 • involuntary reactions of the patient.

246 The diagnosis in most of these situations is currently vague [37][38][39].  
247 The joint investigation of different autonomic responses could help in clar-  
248 ifying the complex dynamics of the ANS in such conditions. One of the  
249 problems when designing an experimental setup is being constrained by the  
250 functionalities of commercial systems, which are usually closed and allow only  
251 specific protocols. Here, we were interested in investigating synchronously  
252 the joint responses of the heart (i.e., the cardiac pulse), the skin (i.e., sweat  
253 production) and pupil. Despite the interest in the study of pupillary dy-  
254 namics, at present there are no tools that are able to simultaneously obtain  
255 the acquisition and processing of pupillary dynamics and those of other sys-  
256 tems such as the cardiovascular (e.g., through pulse oximetry) and sudorific  
257 system (through skin conductivity). Being able to expand the analysis to  
258 several systems in a synchronous way would allow a better knowledge of the  
259 coupling pathways between somatosensory and affective / emotional needs  
260 and responses of the whole of the ANS in physiological and/or pathologi-  
261 cal conditions, probably indicating the activation of different autonomous  
262 circuits in case of different conditions.

263 In this work, we have designed an experimental setup able to record in  
264 synchrony the video of pupil (done with a commercial system [25]) and dif-  
265 ferent responses of the ANS. A modular sensor network was designed and  
266 implemented to acquire, process and transmit via USB some biomedical sig-  
267 nals reflecting the state of the ANS. Two sensors have been included in the  
268 prototype, for pulse oximetry and skin conductivity. However, it is feasible  
269 for being extended to include more body sensors, miniaturized and embedded  
270 in a portable system. This could be important for future extension of the  
271 work, as body sensor networks are finding many applications in the contin-  
272 uous monitoring of sensitive people [40][41][42][43]. Indeed, many different  
273 sensors are available to monitor physiological data and could be included:  
274 accelerometer, blood glucose sensor, electrodes for bioelectric signals, blood

275 pressure sensor, gyroscope, carbon dioxide gas sensor, etc. [44].  
276 The developed system, even if it is only a prototype, provided robust estima-  
277 tions of the electrodermal activity and of the pulse oximetry, which was then  
278 processed to investigate the heart inter-beat interval. Note that the PPG  
279 is immune to electrical artifacts, which could be observed on the electrocar-  
280 diogram during TENS application (however, it is less precise in detecting  
281 the HR, as it also depends on the pulse wave velocity). Thus, our system is  
282 adequate for the study of the ANS response to TENS reflected in the HR.

283 Preliminary experimental tests are shown. Even if we considered only  
284 short recordings, weak ANS stimulations (dental occlusion, light, TENS and  
285 a computational task) in healthy subjects and we extracted simple indexes  
286 (mean, STD and trend), we have shown statistically significant variations of  
287 at least an index in each pair of conditions. This indicates that the overall  
288 information provided by the joint recordings, not just that of each individual  
289 signal, should be used for the discrimination of the ANS responses in the  
290 different considered conditions. The results are in line with our expectations:  
291 HDO and computation elicit the sympathetic response (which should result  
292 in HR and GSR increasing and pupil dilation), TENS induces relaxation  
293 (determining a decrease of HR, GSR and pupil size). Pupil appeared to  
294 be the most sensible system, as it reflected even the small stimuli given by  
295 HDO or TENS. HR showed significant variations only in a few conditions  
296 (e.g., mean HR was significantly increased only by the computation task).  
297 GSR showed an important trend during computation, but it was prone to  
298 accumulation effects (with an average increase along the experiment, in spite  
299 of the application of TENS).

300 Other tests and advanced processing techniques could provide specific in-  
301 dications in physiology or pathology, in future joint acquisitions of different  
302 responses of the ANS. Additional measures to guarantee reproducibility of  
303 the tests need to be developed, such as careful preparation in order to stabi-  
304 lize hemodynamic parameters. Moreover, additional sensors or stimulation  
305 signals could also be included in the proposed device, due to its modular  
306 architecture.

## 307 **References**

- 308 [1] R. Freeman, M. Chapleau, Chapter 7 - testing the autonomic nervous  
309 system, Editor(s): Gérard Said, Christian Krarup, Handbook of Clinical  
310 Neurology 115 (2013) 115–136.

- 311 [2] A. Loewy, M. Spyer, Central regulation of autonomic functions, New  
312 York, United States: Oxford University Press (1990).
- 313 [3] C. Collet, E. Vernet-Maury, G. Delhomme, A. Dittmar, Autonomic ner-  
314 vous system response patterns to basic emotions, *Journal of the Auto-*  
315 *nomous Nervous System* 62 (1997) 45–57.
- 316 [4] D. C. Fowles, M. Christie, R. Edelberg, W. Grings, D. Lykken, P. Ven-  
317 ables, Publication recommendations for electrodermal measurements,  
318 The Society for Psychophysiological Research, Inc. 18 (1981) 232–239.
- 319 [5] C. Lombardi, M. Pengo, G. Parati, Obstructive sleep apnea syndrome  
320 and autonomic dysfunction, *Auton Neurosci.* 221 (2019) 102563.
- 321 [6] M. Kobayashi, N. Tomioka, Y. Ushiyama, T. Ohhashi, Arithmetic cal-  
322 culation, deep inspiration or handgrip exercise-mediated pre-operational  
323 active palmar sweating responses in humans, *Auton Neurosci.* 104 (1)  
324 (2003) 58–65.
- 325 [7] G. Calcagnini, F. Censi, S. Lino, S. Cerutti, Spontaneous fluctuations  
326 of human pupil reflect central autonomic rhythms, *Journal of Methods*  
327 *of Information in Medicine* 39 (2000) 142–145.
- 328 [8] L. Mesin, A. Monaco, R. Cattaneo, Investigation of nonlinear pupil dy-  
329 namics by recurrence quantification analysis, *BioMed Research Interna-*  
330 *tional* 420509 (2013).
- 331 [9] L. Mesin, R. Cattaneo, A. Monaco, E. Pasero, Pupillometric study of  
332 the dysregulation of the autonomous nervous system by svm networks,  
333 Editors: R.J. Howlett, Lakhmi C. Jain, *Smart Innovation, Systems and*  
334 *Technologies*, Springer (2013) 107–116.
- 335 [10] A. Monaco, R. Cattaneo, L. Mesin, I. Ciarrocchi, F. Sgolastra, Dys-  
336 regulation of the autonomous nervous system in patients with tem-  
337 poromandibular disorder: a pupillometric study, *Plos One* 7 (9) (2012)  
338 e45424.
- 339 [11] A. Monaco, R. Cattaneo, L. Mesin, E. Fiorucci, D. Pietropaoli, Evalua-  
340 tion of autonomic nervous system in sleep apnea patients using pupillom-  
341 etry under occlusal stress: a pilot study, *Cranio* 32 (2) (2014) 139–147.

- 342 [12] F. Onorati, L. Mainardi, F. Sirca, V. Russo, R. Barbieri, Nonlinear  
343 analysis of pupillary dynamics, *Biomedical Engineering / Biomedizinis-*  
344 *che Technik* 61 (1) (2016) 95–106.
- 345 [13] A. Venkata Sivakumar, M. Kalburgi-Narayana, M. Kuppusamy, P. Ra-  
346 maswamy, S. Bachali, Computerized dynamic pupillometry as a screen-  
347 ing tool for evaluation of autonomic activity, *Neurophysiologie Clinique*  
348 50 (5) (2020) 321–329.
- 349 [14] S. Aminihaajibashi, T. Hagen, M. Foldal, B. Laeng, E. T., Individual  
350 differences in resting-state pupil size: Evidence for association between  
351 working memory capacity and pupil size variability, *Int J Psychophysiol.*  
352 140 (2019) 1–7.
- 353 [15] S. Jainta, T. Baccino, Analyzing the pupil response due to increased  
354 cognitive demand: an independent component analysis study, *Int J Psy-*  
355 *chophysiol.* 77 (1) (2010) 1–7.
- 356 [16] K. Fröder, F. Pittino, G. Dreisbach, How sequential changes in reward  
357 expectation modulate cognitive control: Pupillometry as a tool to mon-  
358 itor dynamic changes in reward expectation, *Int J Psychophysiol.* 148  
359 (2020) 35–49.
- 360 [17] I. Lee, S. Yoon, S. Lee, H. Lee, H. Park, C. Wallraven, Y. Chae, An  
361 amplification of feedback from facial muscles strengthened sympathetic  
362 activations to emotional facial cues, *Auton Neurosci.* 179 (1-2) (2013)  
363 37–42.
- 364 [18] M. Bradley, L. Miccoli, M. Escrig, P. Lang, The pupil as a measure  
365 of emotional arousal and autonomic activation, *Psychophysiology* 45  
366 (2008) 602–607.
- 367 [19] C. Kelbsch, T. Strasser, Y. Chen, B. Feigl, P. Gamlin, R. Kardon,  
368 T. Peters, K. Roecklein, S. Steinhauer, E. Szabadi, A. Zele, H. Wil-  
369 helm, B. Wilhelm, Standards in pupillography, *Front. Neurol.* 10 (2019)  
370 129.
- 371 [20] M. Strauss, *Handwave: Design and manufacture of a wearable wireless*  
372 *skin conductance sensor and housing*, Massachusetts Institute of Tech-  
373 *nology. Department of Mechanical Engineering* (2005).

- 374 [21] L. de Jesus, J. Rosana, M. Tristao, H. Storm, A. da Rocha, D. Cam-  
375 pos, Heart rate, oxygen saturation, and skin conductance: a comparison  
376 study of acute pain in brazilian newborns, 33rd Annual International  
377 Conference of the IEEE EMBS. Boston, Massachusetts (2011).
- 378 [22] D. Li, H. Zhao, S. Dou, A new signal decomposition to estimate breath-  
379 ing rate and heart rate from photoplethysmography signal, Biomedical  
380 Signal Processing and Control 19 (2015) 89 – 95.
- 381 [23] S. Ghiasi, A. Greco, R. Barbieri, E. Scilingo, G. Valenza, Assessing au-  
382 tonomic function from electrodermal activity and heart rate variability  
383 during cold-pressor test and emotional challenge, Sci Rep. 10 (1) (2020)  
384 5406.
- 385 [24] K. Khalfallah, H. Ayoub, J. Calvet, X. Neveu, P. Brunswick, S. Griveau,  
386 V. Lair, M. Cassir, F. Bedioui, Noninvasive galvanic skin sensor for  
387 early diagnosis of sudomotor disfunction: application to diabetes, IEEE  
388 Sensors Journal 12 (3) (2012) 456–463.
- 389 [25] S. Amplifon, Oculus: Video-oculoscopio digitale.,  
390 www.biomedica.amplifon.com (2012).
- 391 [26] E. Gil, M. Orini, R. Bailón, J. Vergara, L. Mainardi, P. Laguna, Pho-  
392 toplethysmography pulse rate variability as a surrogate measurement of  
393 heart rate variability during non-stationary conditions, Physiol. Meas.  
394 31 (2010) 1271–1290.
- 395 [27] M. Nitzany, A. Babchenko, B. Khanokhy, D. Landau, The variability of  
396 the photoplethysmographic signal- a potential method for the evaluation  
397 of the autonomic nervous system, Physiol. Meas. 19 (1998) 93–102.
- 398 [28] E. Rodrigues, R. Godina, C. Cabrita, J. Catalao, Experimental low cost  
399 reflective type oximeter for wearable health systems, Biomedical Signal  
400 Processing and Control 31 (2017) 419–433.
- 401 [29] O. Fathabadi, T. Gale, J. Olivier, P. Dargaville, Automated control of  
402 inspired oxygen for preterm infants: What we have and what we need,  
403 Biomedical Signal Processing and Control 28 (2016) 9 – 18.
- 404 [30] M. Dawson, A. Schell, D. Filion, The electrodermal system, Handbook  
405 of Psychophysiology. United States: Cambridge University Press (2000).

- 406 [31] T. Reinhardt, C. Schmahl, S. Wust, M. Bohus, Salivary cortisol,  
407 heart rate, electrodermal activity and subjective stress responses to the  
408 mannheim multicomponent stress test (mmst), *Psychiatry Res.* 198 (1)  
409 (2012) 106–111.
- 410 [32] M. Benedek, C. Kaernbach, A continuous measure of phasic electroder-  
411 mal activity, *Journal of Neuroscience Methods* 190 (2010) 80–91.
- 412 [33] Atmel, 8-bit avr microcontroller with 16k bytes in-system programmable  
413 flash: Atmega16, [www.atmel.com](http://www.atmel.com) (2012).
- 414 [34] Atmel, Parametric search of avr microcontrollers, [www.atmel.com](http://www.atmel.com)  
415 (2012).
- 416 [35] R. Tarjan, Depth-first search and linear graph algorithms, *Siam J Com-*  
417 *put.* 1 (1972) 146–160.
- 418 [36] T. Chelimsky, D. Robertson, G. Chelimsky, Disorders of the auto-  
419 nomic nervous system, Daroff: *Bradley’s Neurology in Clinical Practice.*  
420 Philadelphia, United States: Saunders Elsevier (2012).
- 421 [37] H. Chen, A. Nackley, V. Miller, L. Diatchenko, W. Maixner, Multisys-  
422 tem dysregulation in painful temporomandibular disorders, *J Pain* 14  
423 (2012) 983–996.
- 424 [38] W. Maixner, J. Greenspan, R. Dubner, E. Bair, F. Mulkey, V. Miller,  
425 C. Knott, G. Slade, R. Ohrbach, L. Diatchenko, F. R.B., Potential au-  
426 tonomic risk factors for chronic tmd: Descriptive data and empirically  
427 identified domains from the oppera case-control study, *J Pain* 12 (11  
428 Suppl) (2011) T75–T91.
- 429 [39] A. Zygmunt, J. Stanczyk, Methods of evaluation of autonomic nervous  
430 system function, *Arch Med Sci.* 6 (2010) 11–18.
- 431 [40] U. Anliker, J. Ward, P. Lukowicz, G. Troster, F. Dolveck, M. Baer,  
432 F. Keita, E. Schenker, F. Catarsi, L. Coluccini, A. Belardinelli, D. Shk-  
433 larski, M. Alon, E. Hirt, R. Schmid, M. Vuskovic, Amon: a wearable  
434 multiparameter medical monitoring and alert system, *IEEE Trans Inf*  
435 *Technol Biomed.* 8 (2004) 415–427.

- 436 [41] S. Lee, S. Jung, C. Lee, K. Jeong, G. Cho, S. Yoo, Wearable ecg mon-  
437 itoring system using conductive fabrics and active electrodes, Lecture  
438 Notes in Computer Science 5612 (2009) 778–783.
- 439 [42] H. Darwish, Wearable and implantable wireless sensor network solutions  
440 for healthcare monitoring, Sensors 12 (2012) 12375–12376.
- 441 [43] J. Choi, B. Beena Ahmed, R. Gutierrez-Osuna, Development and evalu-  
442 ation of an ambulatory stress monitor based on wearable sensors, IEEE  
443 Transactions On Information Technology In Biomedicine 16 (2) (2012)  
444 279–286.
- 445 [44] M. Chen, S. Gonzalez, A. Vasilakos, H. Cao, V. Leung, Body area net-  
446 works: A survey, Mobile Netw Appl 16 (2011) 171–193.

CONDITIONS	INDEXES with SIGNIFICANT DIFFERENCE
<b>Computation</b> versus <b>RP (D)</b>	<i>Mean HR</i> (p=0.0002) Comp.: 1.4(1.17, 2.04) – RP: 1.08(0.94, 1.57) <i>STD of HR</i> (p=0.001) Comp.: 0.28(0.17, 0.54) – RP: 0.11(0.08, 0.38) <i>STD of GSR</i> (p=0.0015) Comp.: 1.25(0.54, 2.77) – RP: 0.2(0.1, 1.0) <i>Trend of GSR</i> (p=0.0078) Comp.: 3.03(0.27, 3.28) – RP: –0.12(–1.88, 2.06) <i>Mean pupil area</i> (p=0.01) Comp.: 6952(6180, 9050) – RP: 6565(5839, 8072)
<b>HDO (D)</b> versus <b>RP (D)</b>	<i>Mean pupil area</i> (p=0.0029) HDO: 6817(6318, 8636) – RP: 6565(5839, 8072) <i>Trend of pupil area</i> (p=0.012) HDO: 1.05(–0.62, 1.86) – RP: 2.10(1.55, 2.63) <i>STD of pupil area</i> (p=0.024) HDO: 177(142, 279) – RP: 267(202, 308)
<b>pre-TENS</b> versus <b>TENS</b>	<i>Mean of pupil area</i> (p=0.009) pre: 6425(3806, 7391) – tens: 5818(3134, 7082) <i>STD of GSR</i> (p=0.031) pre: 0.11(0.05, 0.27) – tens: 0.21(0.72, 0.83) <i>STD of HR</i> (p=0.036) pre: 0.11(0.07, 0.24) – tens: 0.12(0.09, 0.57)
<b>TENS</b> versus <b>post-TENS</b>	<i>Mean of GSR</i> (p=0.0001) tens: 12.91(9.09, 14.83) – post: 13.65(12.86, 16.61)
<b>pre-TENS</b> versus <b>post-TENS</b>	<i>Mean of GSR</i> (p=0.006) pre: 12.88(10.88, 13.68) – post: 13.65(12.73, 16.61) <i>Mean area of pupil</i> (p=0.012) pre: 6425(3806, 7392) – post: 5823(3151, 6874) <i>STD of HR</i> (p=0.022) pre: 0.12(0.08, 0.25) – post: 0.16(0.08, 0.35)
<b>Light</b> versus <b>Darkness</b>	<i>Mean area of pupil</i> (p<<0.001) L: 2987(2545, 3981) – D: 7312(6613, 9059) <i>STD of pupil</i> (p<<0.001) L: 417(333, 539) – D: 220(161, 283) <i>Trend of pupil</i> (p=0.014) L: 0.23(–0.79, 1.29) – D: 1.70(0.21, 2.32)

Table 2: Statistical analysis of the data using Wilcoxon sign rank test. Mean, standard deviation and trend of data were considered (L: light; D: darkness). Median and quartiles of the indexes showing significant differences (p<0.05) are reported (in order of increasing p). Pupil size is indicated in pixels, HR in Hz, GSR in  $\mu$ S; their trends are measured in arbitrary units (they were computed on normalized data and time).